

Fenton Degradation of Organic Pollutants in the Presence of Low-Molecular-Weight Organic Acids: Cooperative Effect of Quinone and Visible Light

JIAHAI MA, WANHONG MA, WENJING SONG, CHUNCHENG CHEN, YALIN TANG, AND JINCAI ZHAO*

Key Laboratory of Photochemistry, Center for Molecular Science, Institute of Chemistry, The Chinese Academy of Sciences, Beijing 100080, China

YINGPING HUANG

Research Center for Eco-Environmental Sciences, China Three Gorges University, Yichang, Hubei 443002, China

YIMING XU

Department of Chemistry, Zhejiang University, Hangzhou, Zhejiang 310027, China

LING ZANG

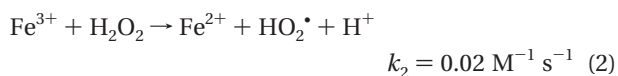
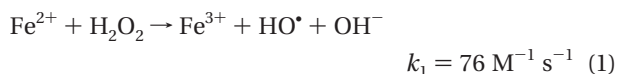
Department of Chemistry and Biochemistry, Southern Illinois University, Carbondale, Illinois 62901

The influence of low-molecular-weight organic acids (LMWOAs), such as malonic acid, ethylenediaminetetraacetic acid, and oxalic acid, on the Fenton degradation of organic pollutants was examined under visible irradiation ($\lambda > 450$ nm). The Fenton degradation of malachite green in the dark was completely blocked in the presence of LMWOAs. It was found that either visible light irradiation or the addition of hydroquinone could initiate the dye degradation, but the mineralization yield was almost zero. An important result was that the dye mineralization in the presence of LMWOAs could be achieved when both visible irradiation and hydroquinone were introduced. Similar results were obtained with colorless pollutants, such as benzyltrimethylammonium chloride and 2,4,5-trichlorophenol. We concluded that coupling visible irradiation and hydroquinone could be a strong and universal driving force in the Fenton reaction for the complete degradation and mineralization of organic pollutants, even in the presence of LMWOAs.

Introduction

The Fenton reaction ($\text{H}_2\text{O}_2 + \text{Fe}^{2+}/\text{Fe}^{3+}$) has been widely used to oxidize and mineralize organic compounds for various purposes, such as wastewater treatment (1, 2), hydroxylation of benzenes and oxygen atom transfer in organic synthesis (3, 4), and DNA damage by free radicals in vivo (5–7). Many researchers have studied the reaction mechanism and kinetics (8–11), but the nature of the reactive species is still a matter of debate (HO^\bullet vs ferryl species) (12–18).

Production of HO^\bullet and other reactive species in the Fenton reaction has been proven by ESR (electron spin resonance) technique, hydroxylation of probe molecules, and kinetic models (4, 19). The general mechanism for a free radical chain is outlined below (9, 20, 21); the reaction (2) is slow and taken as the rate-determining step of the Fenton reaction chain. Among the active species involved, HO^\bullet is considered

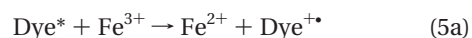
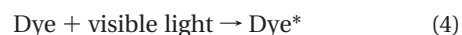


the most reactive one to attack the substrate. Although HO^\bullet is a powerful species ($E^\circ = +2.59\text{V}$ vs NHE) (14) which can nonselectively react with most organics, the Fenton reaction could not reach deep mineralization of target pollutants (usually less than 50% CO_2 yield). The final products formed are usually low-molecular-weight organic acids (LMWOAs), such as oxalic, malonic, and acetic acids (1, 14, 22–24). Consistent with this is that the Fenton's reagent is powerful at initial stage and gradually loses its capability for organic destruction with reaction time (25). It is commonly accepted that such deactivation is due to the interaction of Fe^{3+} with LMWOAs (the degradation intermediates), which is unfavorable to either $\text{Fe}^{3+}/\text{Fe}^{2+}$ recycling (26, 27) or to HO^\bullet generation (28), although the exact mechanism is still obscure. If this is the case, effective circumvention of the blockage of these LMWOA intermediates by an appropriate pathway may improve the iron cycle and achieve continuous production of HO^\bullet for target pollutant mineralization.

Diverse efforts have been made to utilize the Fenton reaction in better ways. The Fenton reaction can be greatly accelerated by UV light irradiation, due to photolysis of ferric species, which enhances the regeneration of Fe^{2+} with concomitant production of HO^\bullet (denoted as the photo-Fenton reaction) (22). In the UV photo-Fenton reaction, 100% of mineralization of organic compounds can be achieved (22, 24).



The UV region is only 3–5% of the total solar spectrum; therefore, it is important to utilize the visible light (the majority of the sunlight) for the Fenton system. However, visible irradiation cannot lead to a reaction (3) since the absorption wavelength of Fe(OH)^{2+} species is < 400 nm. Under visible light irradiation, deep mineralization of organic dyes has been observed due to electron transfer from the excited dye into Fe^{3+} , leading to the catalytic cycling of $\text{Fe}^{3+}/\text{Fe}^{2+}$ (eqs 4–5a) (29–31). Little is known, however, about the reaction of small organic molecules in the Fenton system under visible irradiation. In addition, it was found that the



addition of hydroquinone/quinone analogues could significantly catalyze the Fenton degradation of organic substrates and accelerate the iron cycle (32–34).

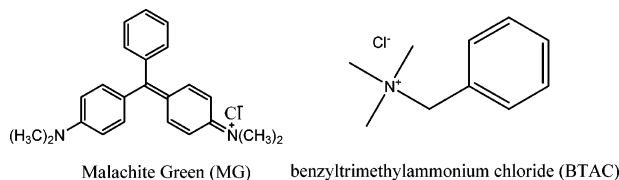
In this work, we have examined the Fenton degradation of organic pollutants under visible irradiation ($\lambda > 450$ nm) in the presence of LMWOAs, which are recalcitrant species

* Corresponding author phone: +86-10-8261-6495; fax: +86-10-8261-6495; e-mail: jczhao@iccas.ac.cn.

in the Fenton reaction. The organic dye malachite green (MG), colorless benzyltrimethylammonium chloride (BTAC), and 2,4,5-trichlorophenol (TCP) were employed as model pollutants. The objective of the present work is to study the various effects of LMWOAs, quinones, and visible irradiation on the reaction pathway in the Fenton reactions. Furthermore, this work will also give insight into the role of HO[•] in the degradation and mineralization of organic pollutants so as to better understand the Fenton chemistry.

Experimental Section

Materials. Malachite green (MG), 2,4,5-trichlorophenol (TCP), and the spin trap reagent, 5,5-dimethyl-1-pyrroline-*N*-oxide (DMPO), were from Sigma. Fe(ClO₄)₃ and HClO₄ were from Aldrich. Benzyltrimethylammonium chloride (BTAC), 1,4-hydroquinone, 1,4-benzoquinone, malonic acid, ethylenediaminetetraacetic acid (EDTA), and methanol and hydrogen peroxide (30%) were of analytical grade. All the chemicals were used as received except where noted. Deionized water was distilled and purified further in a Barnstead Nanopure system to a resistivity greater than 18 MΩ-cm.



Reaction Procedures. All experiments were conducted in a cylindrical Pyrex (Corning, Inc.) vial (50 mL or 100 mL) under magnetic stirring in an aerated solution at an initial pH of 2.90 (adjusted with HClO₄). All the solutions were prepared fresh daily. The stock solution of Fe³⁺ (10 mM) was prepared in 0.1 M HClO₄. The light source was a 500 W halogen lamp (Institute of Electric Light Source, Beijing) positioned inside a cylindrical Pyrex jacket and cooled by circulating water. A cutoff filter at 450 nm was placed outside the Pyrex jacket to ensure that the irradiation consisted of visible light only. The UV light irradiation was from a 100 W Hg lamp (λ > 330 nm, Toshiba SHLS-1002A).

Analysis. At given reaction time intervals, samples were taken out and immediately analyzed on a Hitachi U-3100 UV-vis spectrophotometer for UV-vis spectra. The reaction kinetics for MG degradation was determined by measuring its absorbance change at 617 nm with time. BTAC, 1,4-hydroquinone, and 1,4-benzoquinone were analyzed by HPLC on a Dionex P580 (5 μm, 250 × 5 mm Diamonsil C-18 column) equipped with a built-in UVD 340s diode array UV-vis detector. The mobile phase was 60% methanol and 40% water for BTAC analysis (monitored at 215 nm; retention time, *t_R*, of 2.0 min), 50% methanol and 50% water for analysis of 1,4-hydroquinone (monitored at 290 nm; *t_R* = 3.3 min) and 1,4-benzoquinone (monitored at 250 nm; *t_R* = 4.3 min). All the mobile phases were at 1.0 mL/min, and the water effluent contained 0.1% H₃PO₄. The TOC (total organic carbon) was measured on a Tekmar Dohrmann Apollo 9000 TOC analyzer. All the samples were analyzed immediately to avoid further reactions.

Electron spin resonance (ESR) experiments were performed at room temperature on a Bruker EPR ELEXSYS 500 spectrometer equipped with an in situ irradiation source (a Quanta-Ray ND:YAG laser system λ = 532 nm), and the same quartz capillary tube was used for all the measurements to minimize errors. The ESR instrument was operated with the following parameters: microwave frequency 9.78 GHz, microwave power 0.02 W, and modulation frequency 100 kHz.

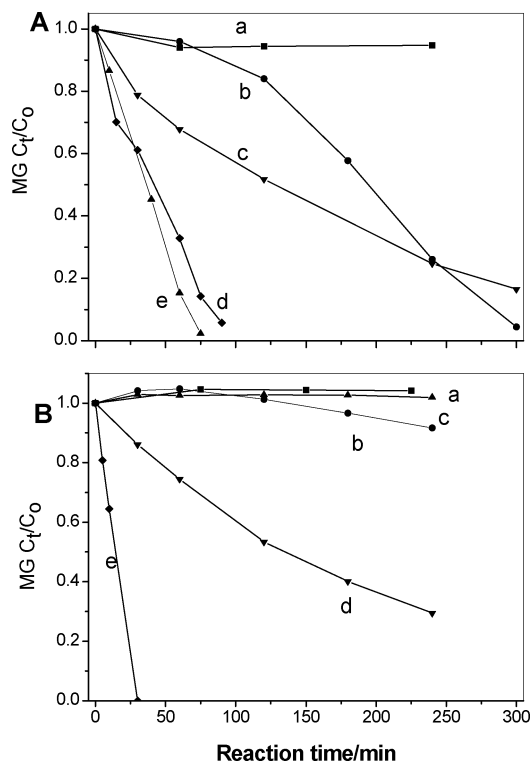
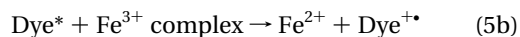


FIGURE 1. Fenton degradation of MG in the presence of (A) malonic acid and (B) EDTA: (a) in the dark, (b) under visible irradiation, (c) in the presence of hydroquinone in the dark, (d) in the presence of hydroquinone under visible irradiation, (e) under UV irradiation. Initial concentrations for (A): 1×10^{-5} M Fe³⁺; 1×10^{-2} M H₂O₂; 5×10^{-5} M malonic acid; 2×10^{-5} M hydroquinone; 2×10^{-5} M MG. Initial concentrations for (B): 2×10^{-4} M Fe³⁺; 2×10^{-3} M H₂O₂; 2×10^{-5} M hydroquinone; 2×10^{-5} M MG; 5×10^{-4} M EDTA.

Results and Discussion

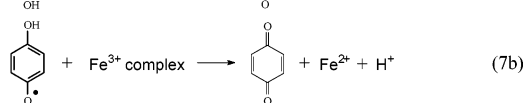
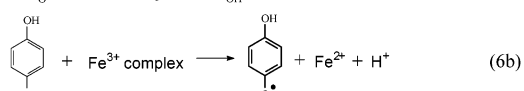
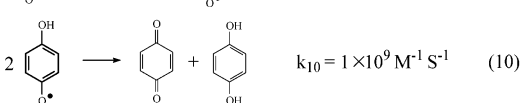
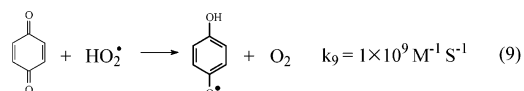
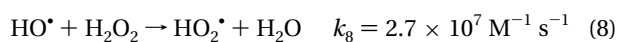
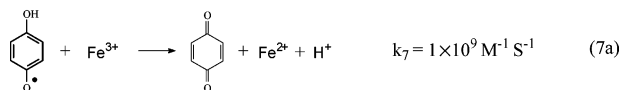
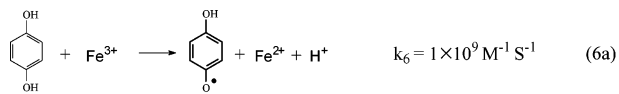
Fenton Degradation of MG in the Presence of Malonic Acid and EDTA. To test whether the formed LMWOAs would block the Fe³⁺/Fe²⁺ cycle and, consequently, depress the substrate degradation, we examined the Fenton degradation of MG in the presence of malonic acid and EDTA (Figure 1A,B), respectively.

Although the Fenton degradation of MG in the dark could easily occur (29, 33), such degradation was not observed in the presence of malonic acid (Figure 1A, curve a). When the solution was irradiated by visible light, the MG degradation occurred continuously in the presence of malonic acid (Figure 1A, curve b). We have reported earlier that the Fenton degradation of organic dyes can be greatly accelerated under visible light irradiation, due to electron transfer from the excited dye into Fe³⁺ species (eqs 4–5a) (29, 30). A similar pathway could be then proposed here for the observed degradation of MG in the presence of malonic acid. The excited dye, MG*, has a redox potential of $E^\circ(\text{MG}^*/\text{MG}^+) = -1.08$ V vs NHE (29), whereas the Fe³⁺–malonic acid complex in the ground state has a redox potential of $E^\circ(\text{Fe}^{3+}/\text{Fe}^{2+}/\text{malonic acid}) = 0.431$ V vs NHE (35). Such energetics favors the electron transfer from MG* to Fe³⁺/malonic acid complex (eq 5b), and the resulting Fe²⁺ species then reacts with H₂O₂ to give HO[•] (eq 1), leading to the degradation of target pollutant MG.



The Fenton degradation of MG in the presence of malonic acid could be also initiated by the addition of hydroquinone in the dark or under visible irradiation (Figure 1A, curve c,d).

In a previous report, we have demonstrated that the addition of hydroquinone could significantly catalyze the Fenton degradation of MG (33). In that system, Fe^{3+} was quickly reduced to Fe^{2+} (eqs 6a and 7a), and the rapid regeneration of Fe^{2+} was achieved bypassing the slow step of the Fenton reaction (eq 2). Meanwhile, the resulting quinone can rapidly react with HO_2^{\bullet} , generated through the Fenton reaction, to regenerate hydroquinone (eqs 8–10), building up the quinone cycle. In the present case, hydroquinone, which has a redox potential of $E^{\circ}(\text{quinone}/\text{hydroquinone}) = 0.30 \text{ V vs NHE}$ (32), can also energetically react with Fe^{3+} –malonic acid complex to produce Fe^{2+} (eqs 6b and 7b), and the resulting Fe^{2+} then reacts with H_2O_2 (eq 1) to sustain the Fenton cycle.



The degradation of MG in the presence of malonic acid became much faster when both hydroquinone and visible irradiation were introduced (Figure 1A, curve d). This reaction was also much faster than the photoreaction in the absence of hydroquinone (Figure 1A, curve b).

We then extended this study using EDTA as an extreme LMWOA, since it can strongly complex the iron species. When EDTA was present, no degradation of MG was observed in the dark or under visible irradiation (Figure 1B, curves a and b). When hydroquinone was added, the degradation of MG still did not occur in the dark (Figure 1B, curve c); note that a similar result was obtained when hydroquinone was replaced by quinone. It was reported that EDTA could retard the Fe-catalyzed oxidation of benzoylformic acid by H_2O_2 (36). Walling also observed that the Fenton oxidation of organic substrates (including bound and free EDTA) was retarded by excess EDTA (9). Energetically, the excited dye, MG^* , was able to inject its electron to Fe^{3+} –EDTA ($E^{\circ}(\text{Fe}^{3+}/\text{Fe}^{2+}$ –EDTA) = 0.12 V vs NHE). The lack of dye degradation actually observed here was probably due to the strong complexation of EDTA with both Fe^{3+} and Fe^{2+} . When oxalic acid was used instead of EDTA, the Fenton degradation of MG in the dark was also not observed, even in the presence of hydroquinone (data not shown), similarly ascribed to the high kinetic stability of iron(III) tris(oxalate) complex. An early study reported that almost no oxalic acid was decomposed by the Fenton reaction in the dark (the molar ratio of Fe^{3+} to oxalic acid was 4:1) (28). Whereas the degradation of MG in the presence of both EDTA and hydroquinone (or

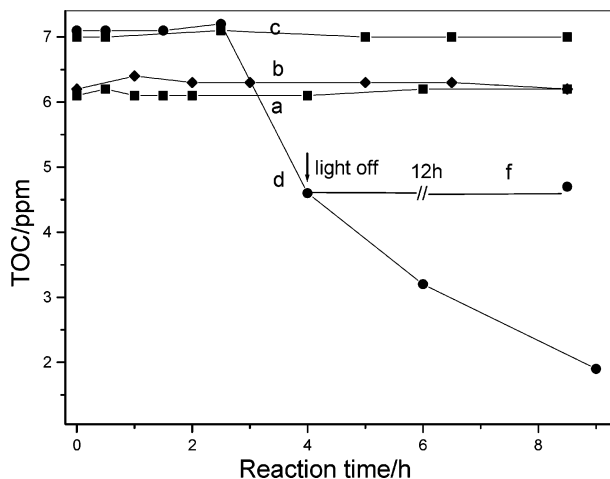


FIGURE 2. Corresponding Fenton mineralization of MG in the presence of malonic acid for Figure 1: (a) in the dark, (b) under visible irradiation, (c) in the presence of hydroquinone in the dark, (d) in the presence of hydroquinone under visible irradiation, (e) the same as d, light off at 4 h time point. Initial concentrations: $1 \times 10^{-5} \text{ M Fe}^{3+}$; $1 \times 10^{-2} \text{ M H}_2\text{O}_2$; $5 \times 10^{-5} \text{ M malonic acid}$; $2 \times 10^{-5} \text{ M MG}$; $2 \times 10^{-5} \text{ M hydroquinone}$ (for c, d, and f).

quinone) did not occur in the dark, the degradation could proceed under visible irradiation (Figure 1B, curve d) (note that the reaction rate in the presence of quinone was somewhat slower than that in the presence of hydroquinone). This evidence suggests that hydroquinone and/or quinone under visible irradiation are able to recycle $\text{Fe}^{2+}/\text{Fe}^{3+}$ via the Fe–EDTA complex, sustaining the Fenton cycle, similar to the result obtained above in the presence of malonic acid (Figure 1A). This indicates that there must be a reaction pathway related with the excited hydroquinone or quinone by visible light (see below).

It was noted that, under UV irradiation, the MG degradation occurred efficiently, even in the presence of EDTA (Figure 1B, curve e). MG itself was stable to UV irradiation. The concentration of free Fe^{3+} species in the reaction system accounted for only about ca. $6.3 \times 10^{-15} \text{ M}$. Thus the observed degradation of MG was due to direct photolysis of Fe^{3+} –EDTA complex under UV irradiation, rather than that of the hydrated Fe^{3+} .

Fenton Mineralization of MG in the Presence of Malonic Acid. It was shown above that the Fenton degradation of MG in the presence of malonic acid could happen under visible irradiation or in the presence of hydroquinone in the dark. Surprisingly, no mineralization was observed under such conditions (Figure 2). That is to say that, in both the cases, only selective oxidation of MG occurred. This was distinct from the Fenton or photo-Fenton degradation of the dye performed in the absence of malonic acid, where partial mineralization in the dark or complete mineralization under visible irradiation was observed. However, deep mineralization of MG was found after 9 h when both visible irradiation and hydroquinone were cooperatively present (Figure 2, curve d). Theoretically, the percentage of TOC from MG, malonic acid, and hydroquinone under the present conditions was 63%, 21%, and 16%, respectively; the major TOC reduction here must come from the mineralization of MG. When the photo-Fenton reaction was performed with malonic acid alone, no mineralization happened and, in the presence of hydroquinone, the TOC value decreased first and leveled to the point before hydroquinone was added, which was attributed to mineralization of the added hydroquinone. That is, malonic acid itself could not be mineralized under the experimental conditions examined. But it is worthy to note that malonic acid could be mineralized to CO_2 when the

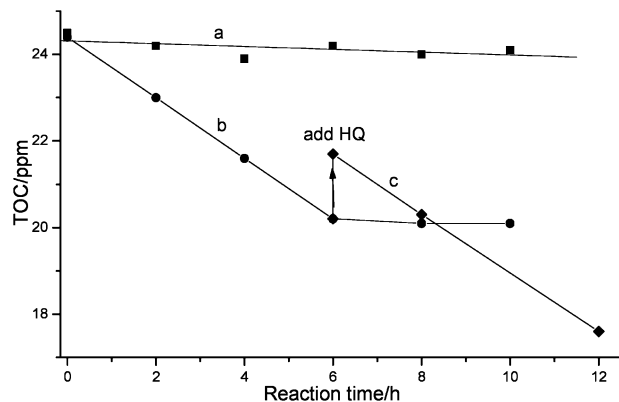


FIGURE 3. Fenton degradation of BTAC in the presence of malonic acid and hydroquinone: (a) in the dark, (b) under visible irradiation, (c) 1×10^{-5} M hydroquinone resupply at arrow (after 6 h). Initial concentrations: 1×10^{-4} M Fe^{3+} ; 2×10^{-2} M H_2O_2 ; 5×10^{-4} M malonic acid; 2×10^{-5} M hydroquinone; 1×10^{-4} M BTAC.

molar ratio of Fe^{3+} to malonic acid was converted, such as 10:1. For practical wastewater treatment, the reaction must be catalytic in iron concentration, and pathways must be available for the regeneration of Fe^{2+} from Fe^{3+} from the influence of the common LMWOAs intermediates in aromatics degradation.

When the light was turned off during the reaction process, the mineralization stopped (Figure 2, curve f). When the initial amount of hydroquinone increased to 8×10^{-5} M from 2×10^{-5} M, the mineralization of MG became much faster under visible irradiation, but still no mineralization was observed in the dark. Recall that visible irradiation, or the addition of hydroquinone, could lead to the degradation of MG in the presence of malonic acid, but only the coupling of both visible irradiation and hydroquinone could make the dye mineralize. Since the presence of hydroquinone caused no MG mineralization but only degradation in the dark, it indicated that the cycle of $\text{Fe}^{3+}/\text{Fe}^{2+}$ driven by hydroquinone could not survive for long if no visible irradiation was introduced. In other words, both visible irradiation and hydroquinone are necessary for the mineralization of MG in the presence of LMWOAs. There was an induction period of about 2.5 h for the mineralization of MG in the presence of LMWOAs and hydroquinone under visible irradiation (the complete discoloration point of MG was 1.5 h, see Figure 1A, curve d).

Fenton Mineralization of BTAC in the Presence of Malonic Acid. To better understand the mechanism and to rule out the effect of visible light excitation of MG, the Fenton degradation of colorless BTAC was investigated in the presence of malonic acid. Although the solution of BTAC, Fe^{3+} , and H_2O_2 has no absorption at the wavelength longer than 400 nm, about 50% of BTAC was mineralized after 6 h of visible light irradiation in the presence of hydroquinone (Figure 3). HPLC analysis showed all BTAC had been transformed after 6 h. Based on the initial molar ratio of hydroquinone to BTAC (1:5) and the mineralization yield (one molecule of hydroquinone gave up two electrons for transformation into quinone, and one molecule of BTAC gave up 53 electrons for complete decomposition into 10 molecules of CO_2), the observed reaction for hydroquinone was a catalytic process rather than a stoichiometric one. After 6 h the mineralization stopped, where hydroquinone was totally consumed. When HQ (1×10^{-5} M) was added, the mineralization went on. The results indicated that both visible irradiation and the presence of hydroquinone are necessary for the mineralization in the Fenton degradation of organic substrates in the presence of LMWOAs.

For TCP, another colorless recalcitrant pollutant, similar results were obtained. Whereas no significant mineralization

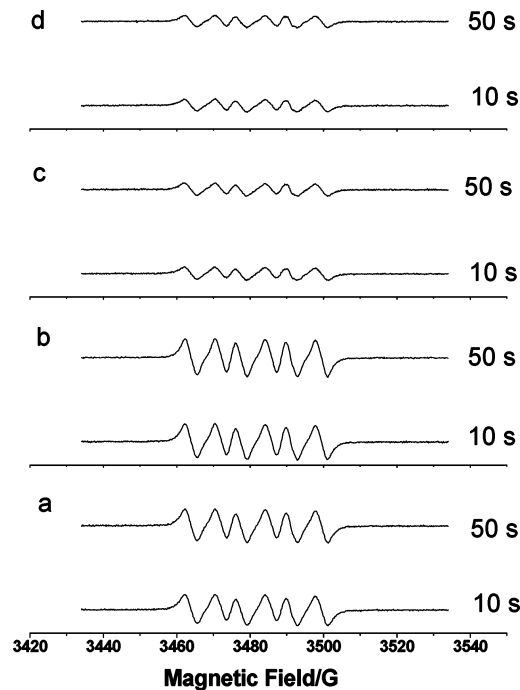


FIGURE 4. Corresponding DMPO-HO_2^* ESR spectra for Figure 1A: (a) in the dark, (b) under visible irradiation, (c) in the presence of hydroquinone in the dark, (d) in the presence of hydroquinone under visible irradiation. Initial concentrations: 1×10^{-5} M Fe^{3+} ; 1×10^{-2} M H_2O_2 ; 5×10^{-5} M malonic acid; 2×10^{-5} M hydroquinone; 2×10^{-5} M MG.

of the target compound was observed in the dark Fenton reaction in the presence of malonic acid and hydroquinone, the irradiation by visible light led to more than 50% of TCP mineralized into CO_2 . From the results, it could be expected that coupling visible irradiation and hydroquinone is a strong and universal driving force in the Fenton reaction for the complete degradation and mineralization of organic pollutants, even in the presence of retarding reagents such as LMWOAs.

Mechanism Discussion

The ESR Results. The role of hydroquinone in the reactions was investigated by the ESR DMPO spin-trap technique (37). It was found that the presence of hydroquinone significantly reduced the signals of DMPO-HO_2^* adduct, whether it was under visible irradiation or not (Figure 4, curves c and d vs curves a and b). Furthermore, almost no DMPO-HO_2^* signals were observed in the absence of malonic acid and in the presence of hydroquinone (data not shown). It meant that HO_2^* was mostly consumed by quinone to give a semiquinone radical, confirming the quinone cycle in the reaction (eq 7). In the case of HO^* (DMPO as scavenger), little signal was observed for the dark Fenton reaction in the presence of malonic acid (Figure 5, curve a), but the characteristic four peaks of DMPO-HO^* adduct appeared for the reaction under the visible irradiation (curve b). Moreover, the intensity of HO^* signals was significantly increased in the presence of hydroquinone either in the dark or under visible irradiation (curves c and d), as compared with reaction b. These results indicated that the presence of malonic acid significantly suppressed the HO^* production, due to its complex with Fe^{3+} . The excited MG under visible irradiation and the presence of hydroquinone were two driving forces making $\text{Fe}^{3+}/\text{Fe}^{2+}$ cycle work and producing HO^* . It seemed that the impact of hydroquinone on MG degradation was much stronger than mere excitation of the dye under visible irradiation.

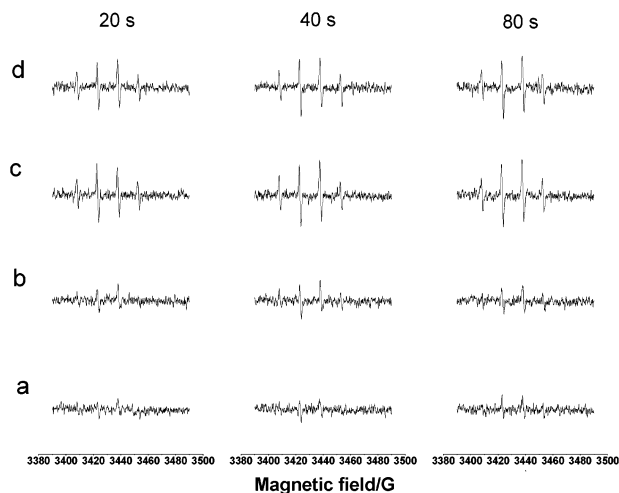


FIGURE 5. Corresponding DMPO–HO• ESR spectra for Figure 1A with the same labels and initial concentrations as Figure 4.

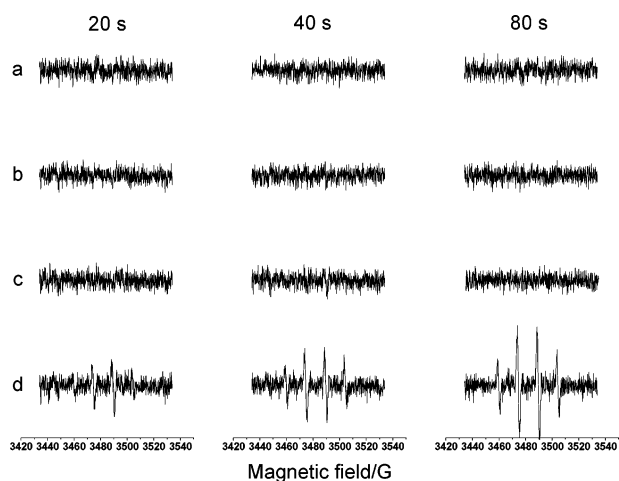


FIGURE 6. The corresponding DMPO–HO• ESR spectra for Figure 1B: (a) in the dark, (b) under visible irradiation, (c) in the presence of hydroquinone in the dark, (d) in the presence of hydroquinone under visible irradiation. Initial concentrations: 2×10^{-4} M Fe^{3+} ; 2×10^{-3} M H_2O_2 ; 2×10^{-5} M hydroquinone; 2×10^{-5} M MG; 5×10^{-4} M EDTA.

The ESR spin-trap technique was also employed to detect the reactive oxygen species in the system containing EDTA. The signals of DMPO–HO• were observed only in the presence of hydroquinone under visible irradiation, as depicted in Figure 6. The signal intensity increased with the irradiation time. For reactions a, b, and c, no HO• was detected, and no degradation of MG took place; for reaction d, HO• was produced, and MG was degraded. It may be inferred that HO• is truly responsible for the Fenton treatment. Furthermore, the presence of hydroquinone also greatly reduced the DMPO–HO₂• signals (Figure 7). The results confirmed that the presence of hydroquinone under visible irradiation was a strong driving force for the Fenton reaction, which steers degradation of target substrates into the desired pathways from the block state of EDTA. The findings provide further evidence that coupling hydroquinone and visible irradiation is decisive on the Fenton degradation of pollutants in the presence of LMWOAs, by looking at EDTA as an extreme LMWOA.

Photolysis of Quinone. As can be seen from the above results, visible irradiation is a necessary factor for efficient degradation and mineralization of organic pollutants by Fenton reaction in the presence of hydroquinone or quinone. We propose that the semiquinone radicals and hydroxyl

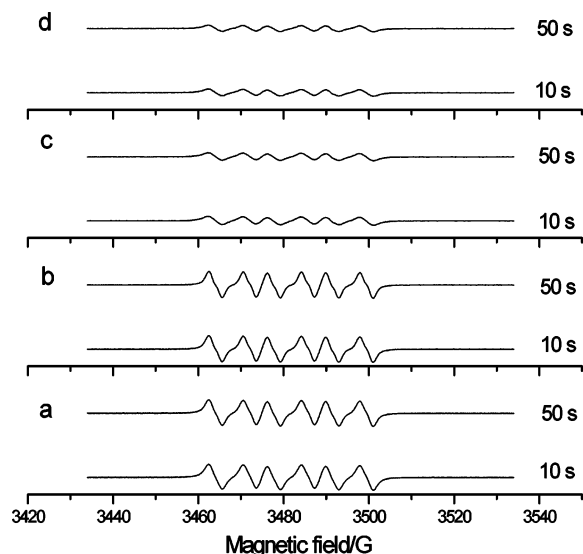


FIGURE 7. Corresponding DMPO–HO₂• ESR spectra for Figure 1B with the same labels and initial concentrations as Figure 6.

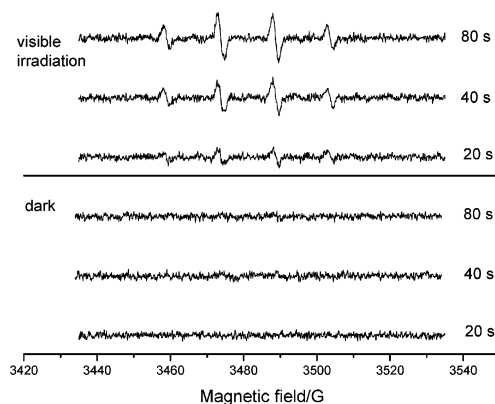
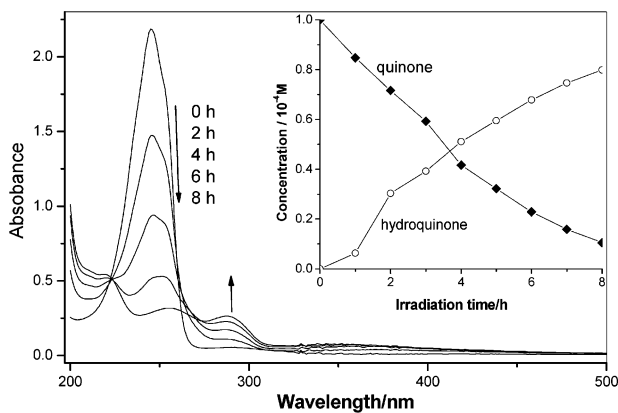
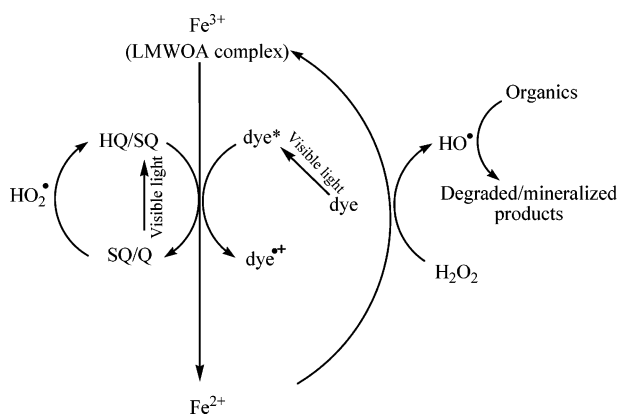


FIGURE 8. Photolysis of 1×10^{-4} M quinone under visible light irradiation at a pH of 2.90. UV/vis spectra change and HPLC concentration profile (above) and the corresponding HO• ESR spectra (below).

radicals are responsible for the observed effect, which are produced by direct photolysis of quinone under visible light irradiation (eq 11) (38).

Figure 8 shows the transformation of quinone under visible irradiation ($\lambda > 450$ nm). Its absorption at 248 nm dropped with the irradiation time, whereas the absorption at around 290 nm rose gradually. Consistent with this, HPLC analysis found about 50% and 80% of hydroquinone accumulation after visible irradiation of quinone for 4 and 8 h, respectively (note that the hydroxyl–benzoquinone was

SCHEME 1. Recycles in Fenton/Photo-Fenton Reactions in the Presence of LMWOAs^a



^a HQ, SQ, and Q denote hydroquinone, semiquinone radical, and quinone, respectively.

not quantitatively monitored due to the lack of a reference standard). At the same time, the ESR signal of HO• appeared and the intensity increased with the irradiation time. The production of semiquinone radical via eq 11 was very important to the quinone transformation pathway, which would greatly promote the Fenton reaction. Furthermore, hydroquinone was mineralized (15% at 1 h and 25% at 2 h) in the dark Fenton reaction (1×10^{-4} M Fe³⁺; 2×10^{-2} M H₂O₂; 8×10^{-5} M hydroquinone), and the mineralization increased under visible irradiation (65.6% at 1 h and 85.8% at 2 h). The higher mineralization ratio confirmed that hydroquinone/quinone transformation pathway was much more facile under visible irradiation.

As can be seen from the above results, in the presence of LMWOAs, (i) the dark Fenton reaction is retarded due to the complex formed with Fe³⁺ and thus stops the Fe²⁺/Fe³⁺ cycle; (ii) introducing the excited dyes under visible irradiation into the system could drive the iron cycle via electron transfer; (iii) addition of hydroquinone makes the pathway to Fe²⁺ available; (iv) the above two driving forces have their limitations: for the first one, when the dye is discolored completely, the force is lost; for the second one, the hydroquinone would also be consumed as a substrate under HO• attack, and the force could not survive too long; (v) hydroquinone, present under visible irradiation in the system, gives another reaction pathway for the quinone cycle besides the HO₂• pathway, and exerts the quinone driving force and, ultimately, the iron recycling is improved.

Furthermore, HO• is involved in all the stages of the Fenton reaction, which would be responsible for the degradation and mineralization of organic pollutants, whereas HO₂• does not directly correspond to mineralization of organics. It has been reported that the HO₂• produced by the well-known Ce(IV)/H₂O₂ reaction was incapable of releasing any CO₂ from the 2,4-D ring (24), which is consistent with the poor reactivity of HO₂• toward organic compounds as compared to HO• (21). No matter what method is used, efficient regeneration of Fe²⁺ from Fe³⁺ or Fe³⁺ complex would maintain the Fenton reaction. Based on all the information obtained above, a possible reaction mechanism in the presence of LMWOAs is proposed in Scheme 1.

As Walling noted, the Fenton-type oxidations of aromatics are particularly complicated and much argument about the oxidant nature in the reactions is risky unless the experimental conditions are exactly specified (12). Based on the above discussions, we consider HO• the most important reactive species that plays the dominating role in the mineralization of organic compounds by Fenton or photo-Fenton reactions. Recycling Fe²⁺ from Fe³⁺ or its complexes dominates HO• production, and it is the primary driving power in the Fenton

reactions. No matter what factor is introduced, the one that can improve the cycle of Fe³⁺ (or its complexes)/Fe²⁺ would promote the Fenton reaction. Better understanding of these reactions is needed for both the study of the reaction mechanism and the successful application of Fenton-type remediation technologies.

Acknowledgments

This work was financially supported under grants from the Ministry of Science and Technology of China (no. 2003CB415006) and the National Science Foundation of China (nos. 20373074, 20537010, 50436040, and 20520120221).

Literature Cited

- Thomas, B.; Philip, H.; Daniel, S.; Fritz, H. F. Photoformation of low-molecular-weight organic acids from brown water dissolved organic matter. *Environ. Sci. Technol.* **2003**, *37*, 4190–4198.
- Casado, J.; Fornaguera, J.; Galan, M. I. Mineralization of aromatics in water by sunlight-assisted electro-Fenton technology in a pilot reactor. *Environ. Sci. Technol.* **2005**, *39*, 1843–1847.
- Ying, Y. M.; Saini, K. R.; Liang, F.; Sadana, K. A.; Billups, E. W. Functionalization of carbon nanotubes by free radicals. *Org. Lett.* **2003**, *5*, 1471–1473.
- Walling, C.; Amarnath, K. Oxidation of mandelic acid by Fenton's reagent. *J. Am. Chem. Soc.* **1982**, *104*, 1185–1189.
- White, B.; Smyth, R. M.; Stuart, D. J.; Rusling, F. J. Oscillating formation of 8-oxoguanine during DNA oxidation. *J. Am. Chem. Soc.* **2003**, *125*, 6604–6605.
- Fukuhara, K.; Nakanishi, I.; Kansui, H.; Sugiyama, E.; Kimura, M.; Shimada, T.; Urano, S.; Yamaguchi, K.; Miyata, N. Enhanced radical-scavenging activity of a planar catechin analogue. *J. Am. Chem. Soc.* **2002**, *124*, 5952–5953.
- Riviere, J.; Bergeron, F.; Tremblay, S.; Gasparutto, D.; Cadet, J.; Wagner, J. R. Oxidation of 5-hydroxy-2'-deoxyuridine into isodialuric acid, dialuric acid, and hydantoin products. *J. Am. Chem. Soc.* **2004**, *126*, 6548–6549.
- Fenton, H. J. H. Oxidation of tartaric acid in the presence of iron. *J. Chem. Soc.* **1894**, *6*, 899–910.
- Walling, C. Fenton's reagent revisited. *Acc. Chem. Res.* **1975**, *8*, 125–131.
- Kunai, A.; Hata, S.; Ito, S.; Sasaki, K. The role of oxygen in the hydroxylation reaction of benzene with Fenton's reagent. ¹⁸O tracer study. *J. Am. Chem. Soc.* **1986**, *108*, 6012–6016.
- Ensing, B.; Buda, F.; Blochl, P.; Baerends J. E. Chemical involvement of solvent water molecules in elementary steps of the Fenton oxidation reaction. *Angew. Chem., Int. Ed.* **2001**, *40*, 2893–2895.
- Walling, C. Intermediates in the reactions of fenton type reagents. *Acc. Chem. Res.* **1998**, *31*, 155–157.
- Goldstein, S.; Meyerstein, D. Comments on the mechanism of the "Fenton-like" Reaction. *Acc. Chem. Res.* **1999**, *32*, 547–550.
- Bossmann, S. H.; Oliveros, E.; Gob, S.; Siegwart, S.; Dahlen, E. P.; Payawan, L., Jr.; Straub, M.; Worner, M.; Braun, A. M. New evidence against hydroxyl radicals as reactive intermediates in the thermal and photochemically enhanced Fenton reactions. *J. Phys. Chem. A* **1998**, *102*, 5542–5550.
- Sawyer, D. T.; Sobkowiak, A.; Matsushita, T. Metal [ML_x; M = Fe, Cu, Co, Mn]/hydroperoxide-induced activation of dioxygen for the oxygenation of hydrocarbons: oxygenated Fenton chemistry. *Acc. Chem. Res.* **1996**, *29*, 409–416 and references therein.
- Pignatello, J. J.; Liu, D.; Huston, P. Evidence for an additional oxidant in the photoassisted Fenton reaction. *Environ. Sci. Technol.* **1999**, *33*, 1832–1839.
- Kremer, L. M. Mechanism of the Fenton reaction. Evidence for a new intermediate. *Phys. Chem. Chem. Phys.* **1999**, *1*, 3595–3605.
- Mekmouche, Y.; Menage, S.; Duboc, T. C.; Fontcave, M.; Galey, J. B.; Lebrun, C.; Pecalet, J. H₂O₂-dependent Fe-catalyzed oxidations: control of the active species. *Angew. Chem., Int. Ed.* **2001**, *40*, 949–952.
- Duesterberg, K. C.; Cooper, J. W.; Waite, D. T. Fenton-mediated oxidation in the presence and absence of oxygen. *Environ. Sci. Technol.* **2005**, *39*, 5052–5058.
- Walling, C.; Goosen, A. Mechanism of the ferric ion catalyzed decomposition of hydrogen peroxide. Effect of organic substrates. *J. Am. Chem. Soc.* **1973**, *95*, 2987–2991.

- (21) Buxton, G. V.; Greenstock, C. L.; Helman, W. P.; Ross, A. B. Critical review of rate constants for reactions of hydrated electrons, hydrogen atoms and hydroxyl radicals in aqueous solution. *J. Phys. Chem. Ref. Data* **1988**, *17*, 513–886.
- (22) Pignatello, J. J. Dark and Photoassisted Fe³⁺-catalyzed degradation of chlorophenoxy herbicides by hydrogen peroxide. *Environ. Sci. Technol.* **1992**, *26*, 944–951.
- (23) Mae, K.; Shindo, H.; Miura, K. A new two-step oxidative degradation method for producing valuable chemicals from low rank coals under mild conditions. *Energy Fuels* **2001**, *15*, 611–617.
- (24) Sun, Y. F.; Pignatello, J. J. Photochemical reactions involved in the total mineralization of 2,4-D by Fe³⁺/H₂O₂/UV. *Environ. Sci. Technol.* **1993**, *27*, 304–310.
- (25) Benitez, F. J.; Heredia, B. J.; Acero, L. J.; Rubio, F. J. Chemical decomposition of 2,4,6-trichlorophenol by ozone, Fenton's reagent, and UV irradiation. *Ind. Eng. Chem. Res.* **1999**, *38*, 1341–1349.
- (26) Fernandez, J.; Dhananjeyan, M. R.; Kiwi, J.; Senuma, Y.; Hilborn, J. Evidence for Fenton photoassisted processes mediated by encapsulated Fe ions at biocompatible pH values. *J. Phys. Chem. B* **2000**, *104*, 5298–5301.
- (27) Rupert, G.; Bauer, R.; Gisler, G. The photo-Fenton reaction - an effective photochemical wastewater treatment process. *J. Photochem. Photobiol., A Chem.* **1993**, *73*, 75–78.
- (28) Sun, Y. F.; Pignatello, J. J. Organic intermediates in the degradation of 2,4-dichlorophenoxyacetic acid by Fe³⁺/H₂O₂ and Fe³⁺/H₂O₂/UV. *J. Agric. Food Chem.* **1993**, *41*, 1139–1142.
- (29) Wu, K. Q.; Xie, Y. D.; Zhao, J. C.; Hidaka, H. Photo-Fenton degradation of a dye under visible light irradiation. *J. Mol. Catal. A: Chem.* **1999**, *144*, 77–84.
- (30) Xie, Y. D.; Chen, F.; He, J. J.; Zhao, J. C.; Wang, H. Photoassisted degradation of dyes in the presence of Fe³⁺ and H₂O₂ under visible irradiation. *J. Photochem. Photobiol., A Chem.* **2000**, *136*, 235–240.
- (31) Herrera, F.; Kiwi, J.; Lopez, A.; Nadtocheko, V. Photochemical decoloration of Remazol Brilliant Blue and Uniblue A in the presence of Fe³⁺ and H₂O₂. *Environ. Sci. Technol.* **1999**, *33*, 3145–3151.
- (32) Chen, R. Z.; Pignatello, J. J. Role of quinone intermediates as electron shuttles in Fenton and photoassisted Fenton oxidations of aromatic compounds. *Environ. Sci. Technol.* **1997**, *31*, 2399–2406.
- (33) Chen, F.; Ma, W. H.; He, J. J.; Zhao, J. C. Fenton degradation of Malachite Green catalyzed by aromatic additives. *J. Phys. Chem. A* **2002**, *106*, 9485–9490.
- (34) Chen, F.; Ma, W. H.; He, J. J.; Zhao, J. C.; Yu, J. C. Photo-Fenton degradation of Malachite Green catalyzed by aromatic compounds under visible irradiation. *New J. Chem.* **2002**, *36*, 336–341.
- (35) Huston, J. T.; Stone, S. A. Reduction of oxamyl and related pesticides by Fe^{II}: influence of organic ligands and natural organic matter. *Environ. Sci. Technol.* **2002**, *36*, 5172–5183.
- (36) Siegel, B.; Lanphear, J. Iron-catalyzed oxidative decarboxylation of benzooylformic acid. *J. Am. Chem. Soc.* **1979**, *101*, 2221–2222.
- (37) Wu, T. X.; Lin, T.; Zhao, J. C.; Hidaka, H.; Serpone, N. TiO₂-assisted photodegradation of dyes. 9. Photooxidation of a squarylium cyanine dye in aqueous dispersions under visible light irradiation. *Environ. Sci. Technol.* **1999**, *33*, 1379–1387.
- (38) Ononye, A. I.; McIntosh, A. R.; Bolton, J. R. Mechanism of the photochemistry of *p*-benzoquinone in aqueous solutions. 1. spin trapping and flash photolysis electron paramagnetic resonance studies. *J. Phys. Chem.* **1986**, *90*, 6266–6270.

Received for review August 21, 2005. Revised manuscript received October 20, 2005. Accepted November 2, 2005.

ES051657T